

Production of Ammonia Using $\text{Sm}_3\text{Fe}_5\text{O}_{12}$ as Nanocatalyst and Its Kinetic Energy Study

by

Andrey Walter Musti

10078

ELECTRICAL & ELECTRONIC ENGINEERING

A Final Report Submitted in Partial Fulfillment of
the Requirement for the
Bachelor of Engineering (Hons)
(Electrical & Electronic Engineering)

May 2011

Universiti Teknologi PETRONAS

Bandar Seri Iskandar

31750 Tronoh

Perak Darul Ridzuan

CERTIFICATION OF APPROVAL

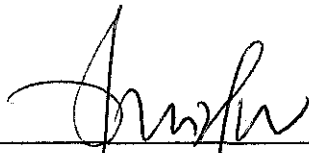
Production of Ammonia Using $\text{Sm}_3\text{Fe}_5\text{O}_{12}$ as Nanocatalyst and Its Kinetic Energy Study

by

Andrey Walter Musti

A Final report submitted to the
Electrical & Electronics Engineering Program
Universiti Teknologi PETRONAS
in partial fulfillment of the requirement for the
Bachelor of Engineering (Hons)
(Electrical & Electronics Engineering)

Approved:



PROF. DR. NOOR HAFIZA A. YAHYA
Professor Dr. Noor Hafiza A. Yahya
Project Supervisor
Faculty of Science & Information Technology
Universiti Teknologi PETRONAS

UNIVERSITI TEKNOLOGI PETRONAS

TRONOH, PERAK

May 2011

CERTIFICATION OF ORIGINALITY

This is to certify that I am responsible for the work submitted in this project, that the original work is my own except as specified in the references and acknowledgements, and that the original work contained herein have not been undertaken or done by unspecified sources or persons.



ANDREY WALTER MUSTI

ABSTRACT

The study for ammonia production has increased since the agriculture industry needs ammonia to produce urea. Current technology in producing ammonia requires very high temperature (300-500°C), high pressure (150-300atm) and high cost which results only 10-20% of total reaction hydrogen and nitrogen gas. This sparks the interest in producing ammonia using nanocatalyst to get the high yield of ammonia. This project focuses on using Samarium Iron Garnet ($\text{Sm}_3\text{Fe}_5\text{O}_{12}$) as a nanocatalyst in producing ammonia. The catalyst was reduced using TPR method and run through nitrogen and hydrogen gas using two types of chamber which are steel and glass chamber. Magnetic field is also applied to observe the changes in the amount of ammonia yield. The results show that the amount of ammonia obtained using Samarium Iron Garnet as nanocatalyst with the presence of magnetic field is 54.8% of the total reaction in ambient condition. The future work for this project is to use CNTs as a support with the nanocatalyst in hope of obtaining higher yield of ammonia.

ACKNOWLEDGEMENT

First and foremost, I would like to thank GOD for giving me the strength and will power to complete this project. I would like to express my deepest gratitude to my supervisor Prof. Dr. Noorhana Yahya for her continuous support and teaching throughout completing this project. She is the backbone of this project which by her abundant knowledge and skills has helped me to grow in term of human being as well as a student. Also, I would love to thank the entire Postgraduate students especially Poppy Puspitasari who plays a big part in making this project a successful one. Lastly, I would like to thank my family members and loved ones for being there when I need them.

TABLE OF CONTENTS

LIST OF FIGURES.....	viii
LIST OF TABLES.....	ix
LIST OF ABBREVIATIONS.....	x
CHAPTER 1 INTRODUCTION.....	1
1.1 Background of study.....	1
1.2 Problem statement.....	2
1.3 Objectives and Scope of Study.....	3
1.3.1 The relevancy of project.....	4
1.3.2 Feasibility of the project.....	4
CHAPTER 2 LITERATURE REVIEW.....	5
2.1 Catalyst for ammonia synthesis.....	5
2.2 Samarium Iron Garnet.....	6
2.3 Haber –Bosch.....	6
2.4 Catalyst support.....	7
2.5 Magnetization.....	8
2.6 Curie Temperature.....	9
2.7 Spin and Activation Energy.....	10

2.8 Arrhenius Kinetic Energy.....	10
2.9 Gibbs Free Energy.....	12
CHAPTER 3 METHODOLOGY.....	15
3.1 Procedure Identification.....	15
3.2 Technical Design.....	17
3.2.1 Micro reactor.....	17
3.2.2 Tools and Equipments.....	17
3.2.2.1 Magnetizer.....	17
3.2.2.2 Kjedahl Method.....	18
3.2.2.3 Tesla Supply.....	19
3.2.2.4 Helmholtz Coil.....	21
CHAPTER 4 RESULTS AND DISCUSSION.....	21
4.1 SaIGs Characterization.....	21
4.2 Ammonia production of SaIG, YIG, and Manganese Zinc Ferrite....	25
CHAPTER 5 CONCLUSION AND RECOMMENDATION.....	38
5.1 Conclusion.....	38
5.2 Recommendation.....	38
REFERENCES.....	40
APPENDICES.....	43

LIST OF FIGURES

Figure 1: Worldwide ammonia production.....	1
Figure 2: Ammonia production by region.....	2
Figure 3: Haber - Bosch process	7
Figure 4: Magnetic alignment	9
Figure 5: Activation energy	12
Figure 6: Gibbs free energy.....	14
Figure 7: Flow chart of the project.....	15
Figure 8: Micro reactor in the lab	17
Figure 9: The magnetization coil	18
Figure 10: (a) Titration pipet; (b) Phenolphthalein; (c) NaOH; (d) Ammonia collection bottle	19
Figure 11: Tesla Power Supply	20
Figure 12: Helmholtz coil	20
Figure 13: XRD profile calcined at different temperature	21
Figure 14: FESEM analysis at different resolutions	23
Figure 15: TPR result of SaIG (detected peak is at 284968 mVs).....	24
Figure 16: The graph shows that the production of ammonia decreases as the temperature increases	26
Figure 17: Comparison between steel and glass chamber	27
Figure 18: Production of ammonia using manganese zinc ferrite.....	29

Figure 19: Production of ammonia against temperature	30
Figure 20: Three nanocatalysts in comparison (with presence of magnetic field)	31
Figure 21: Three nanocatalysts in comparison (with absence of magnetic field).....	32
Figure 22: Arrhenius plot of ammonia production for $\text{Sm}_3\text{Fe}_5\text{O}_{12}$ nanocatalyst with magnetic field. T = 28°C - 188°C, P = 1 atm, Cat. = 0.2g, H ₂ :N ₂ = 3:1..	32
Figure 23: Arrhenius plot of ammonia production for $\text{Sm}_3\text{Fe}_5\text{O}_{12}$ nanocatalyst without magnetic field, T = 28°C - 188°C, P = 1 atm, Cat. = 0.2g, H ₂ :N ₂ = 3:1..	33
Figure 24: Production of ammonia with and without magnetic field	34
Figure 25: Activation energy for yttrium is calculated using the slope	34
Figure 26: Comparison between Helmholtz and magnetizer as the source of magnetic field at room temperature using glass chamber	36
Figure 27: Ammonia yield when CNTs are mix with the catalyst.....	37

LIST OF TABLES

Table 1: Curie temperature of some materials	9
Table 2: TPR for SaIG	23
Table 3: EDX results of SaIG	24
Table 4: Percentage of Ammonia yield with and without Magnetic Field using steel chamber	25
Table 5: Percentage of ammonia yield using Glass Tube at temperature of 28°C	27
Table 6: Percentage of Ammonia yield for Manganese Zinc Ferrite.....	28
Table 7: Amount of Ammonia using YIG	29
Table 8: Activation energy for both garnet materials	35

LIST OF ABBREVIATIONS

SaIG	Samarium Iron Garnet
TPR	Temperature Programmed Desorption Reduction
FESEM	Field Emission Scanning Electron Microscopy
CNTs	Carbon Nanotubes
YIG	Yttrium Iron Garnet

CHAPTER 1

INTRODUCTION

1.1 Background of study

The interest of urea in fertilizer industry has resulted in an increase in the demand of ammonia in a large scale. Friedrich Wohler was the first one to synthesis the urea from inorganic compound in 1828[1]. In 19th century, a method to synthesis urea using ammonia and carbon dioxide was developed.

The production of ammonia was a great discovery and contributed a lot in fundamental science. Until now there are still papers publish on the production of ammonia using various method and parameters.

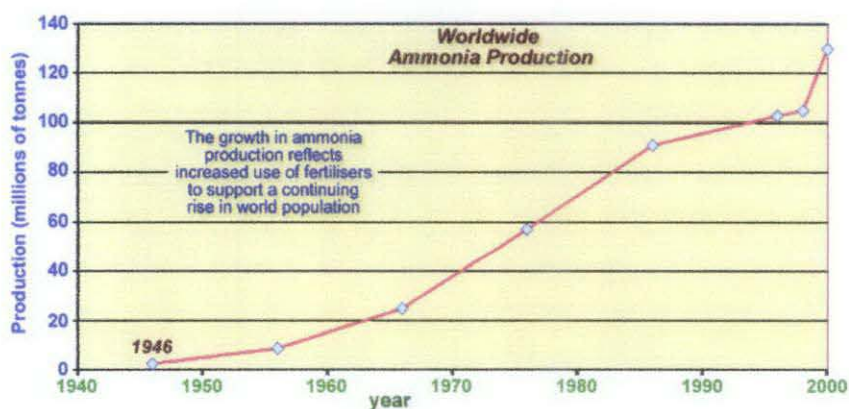


Figure 1: Worldwide ammonia production

Ammonia, the main component for nitrogen fertilizers is produced by combining nitrogen and with hydrogen. Over the past 30 years, the production of ammonia has moved from developed countries to the less developed countries to tackle the world market. The graph below shows the market share by region

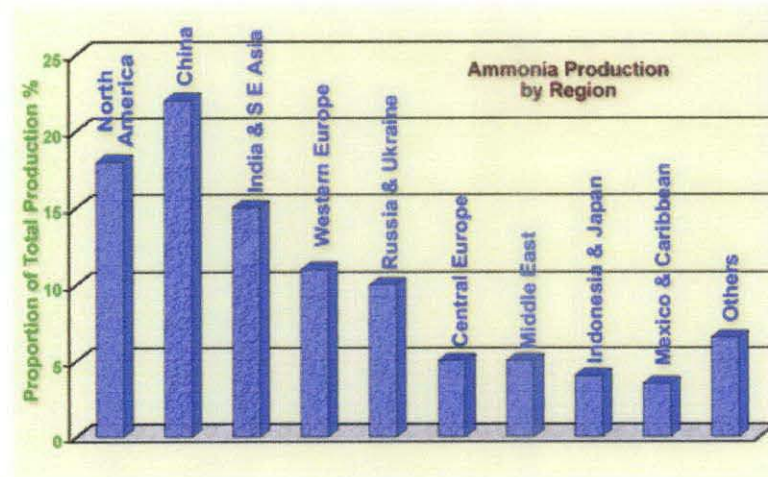


Figure 2: Ammonia production by region

The agriculture industry particularly Malaysia has turned to be an important sector in generating income. This can be seen through the establishment of Petronas Fertilizer Kedah and Petronas Ammonia in Terengganu.

1.2 Problem Statement

The first challenge for this project is to produce ammonia by using a micro reactor. The current production of ammonia requires high pressure (150 – 300 atm),

high temperature (300°C - 500°C), high cost and only 10% - 20% of total reaction of hydrogen and nitrogen can be obtained.

The second challenge for this project is to study the properties of the catalyst which is Samarium Iron Garnet nanocatalyst as well as its kinetic energy properties.

1.3 Objective and Scope of Study

The purpose of this project is to produce ammonia using micro reactor. This is done by using Samarium Iron Garnet as nanocatalyst.

There are several objectives for this project:

- To study the properties of Samarium Iron Garnet and its kinetic energy
- To evaluate the parameters such as temperature and magnetization effect in micro reactor system to maximize the production of ammonia
- To evaluate the type of chamber that can produce higher yield of ammonia

1.3.1 The Relevancy of the Project

This project is relevant to the study of Applied Physics and Applied Chemistry. This project is also relevant to the agricultural and fertilizer industries. With the micro reactor system, the production of ammonia using these catalysts will be study to know the best nanocatalyst to produce higher rate of ammonia. The study and findings of this project will also help in maximizing the production of ammonia.

1.3.2 Feasibility of the Project within the Scope and Time frame

The project will start by doing some research on the current research and experiments done on the production of ammonia. Materials such as journals, books and technical papers regarding the Samarium Iron Garnet, Manganese Zinc Ferrite and Yttrium Iron Garnet properties will be collected as references. Further research will be done from time to time to provide solid findings and progress in studying the catalysts.

CHAPTER 2

LITERATURE REVIEW

2.1 Catalyst for Ammonia Synthesis

Commonly, magnetite (Fe_3O_4) is used as catalyst in ammonia synthesis. It is cooperated with aluminum, potassium, calcium and irreducible oxides [2]. Due to the easy cation substitution for Al^{3+} and Fe^{3+} , the uniform distribution of aluminum in solid can be obtained [3]. A new founding suggested that wustite as a new catalyst in ammonia synthesis [4] has an increase of 30% compared to those obtained from magnetite. Wustite is favourable compared to magnetite due to its ability to be reduced while maintaining its mechanical strength and thermoresistency.

Also ruthenium based catalyst is in favour due to its long term stability and activity also low pressure and temperature condition while producing ammonia [5]. *Ruthenium with potassium metal is suggested as a very effective catalyst which performed greatly under atmospheric pressure [6].* High ammonia yield approximately 40-50% was produced using Ru/C catalyst. The temperature condition and pressure condition are 370-400°C and 50-100 atm respectively [7]. The major disadvantage of this catalyst is its extremely high cost [8].

2.2 Samarium Iron Garnet

Garnet materials such as yttrium or samarium possess unique thermophysical, mechanical and optical properties. Particularly, it has high resistivity on radiation damage, fracture toughness, and energy transfer efficiency. They are widely used in optical communication and magneto – optical devices [9, 10]. Also, SIGs are important due to their wide variety in of magnetic properties by substituting it by other earth material [11 - 15].

2.3 Haber – Bosch Process

This method was founded by Haber - Borsh in 1913. On 19th century, chemists enable to investigate the synthesis of ammonia productively. At normal pressure, the reaction temperature should be kept below 300°C in order to gain a small percentage of ammonia and no catalyst was used. By increasing the pressure to 75 bar the equilibrium conditions enhanced, but the temperature is increase to 600°C. Finally Haber acknowledged that much higher pressures had to be applied and he built a small laboratory apparatus for the continuous production of ammonia. In the early 1909, Haber found distributed osmium, a catalyst which yielded 8% ammonia at 175 bars and about 600°C. He also found that uranium could be used as a catalyst. In July 1909, he demonstrated the production of 80 g of ammonia/hr with this apparatus. The catalyst that Haber used was too expensive to gain any profit. Along with Carl Bosch, Haber invented a large-scale catalytic synthesis of ammonia from elemental hydrogen and nitrogen gas, reactants which are plentiful and cheap. By using high pressure (approximately 150-200 atm), high temperature (around 500°C), and an iron

catalyst, Haber could force relatively unreactive nitrogen and hydrogen gas to mix into ammonia.

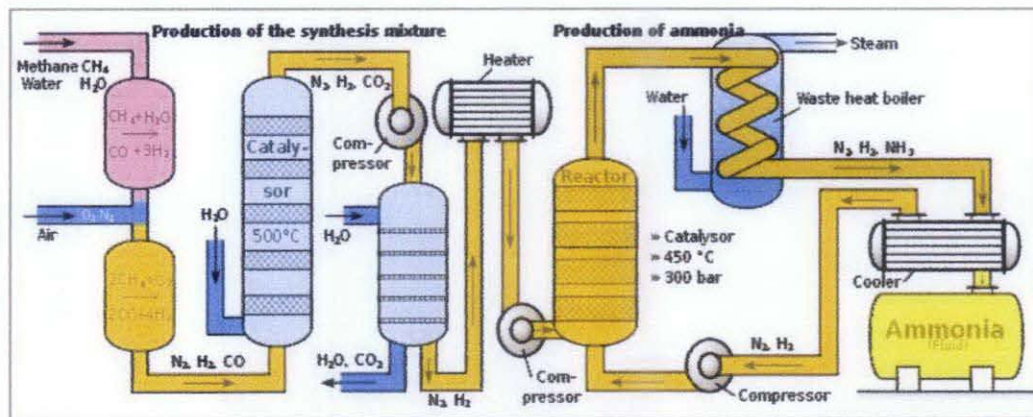


Figure 3: Haber - Bosch process

2.4 Catalyst Support

CNTs as a support have been widely regarded to give higher yield of ammonia due to their properties. Because of their high external surfaces it can give good electronic conductivity. With their large surface to volume ratio due to high external surfaces the possibility to control porosity and surface chemistry of the nanocatalyst increases. Also, CNTs possess very high mechanical properties while maintaining its thermal stability. Table below summarizes some of the catalyst supports that have been used in obtaining higher yield of ammonia.

Table 1: Summary of catalyst support

Catalyst	Who	Results
Ruthenium/Carbon support	British Petroleum Company, cooperated with, M.W. Kellog	<ul style="list-style-type: none">• Produced five to ten times higher reactivity rate (40-50%)• Expensive• High pressure (50-100atm)• High temp(370-400°C)
Ru/CNTs	Yin et. al.	<ul style="list-style-type: none">• High catalytic activity• An increase of 30%

2.5 Magnetization

The magnet alignment called domains is caused by the microscopic ordering of electron spins of ferromagnetic materials [16]. The iron will be magnetized in the direction of the applied magnetic field. With external field, the alignment of the Iron will follow the direction of North to South poles.

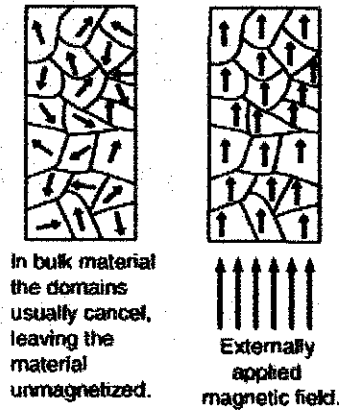


Figure 4: Magnetic alignment

2.6 Curie Temperature

When temperature increases, the magnetization of a ferromagnetic material will lose its magnetism when it reaches Curie point. The phenomenon is called paramagnetic. Below Curie temperature, the neighboring magnetic spins are aligned properly. As the temperature increases, the magnetization (alignment) within each domain decreases so that the magnetic moments become totally disordered. Table below shows some of the Curie temperature of certain materials

Table 2: Curie temperature of some materials

Substances	Curie Temperature (°C)
Iron (Fe)	770
Cobalt (Co)	1130

Nickel (Ni)	358
Iron Oxide (Fe ₂ O ₃)	622

2.7 Spin and Activation Energy

Since the investigation of fractional quantum Hall Effect (FQHE), which is the collective state where the electrons bind together with magnetic flux lines to make a new quasiparticles [17, 18] a lot of experiments were done to study the interactions under strong perpendicular magnetic field [19]. Due to the improved technology, the structure of its ground state or in its excitations can be resolved [20-29].

The energy of the spin-flip like excitations can be measured by measuring the activation energy [30, 31].

2.8 Arrhenius Kinetic Energy

Arrhenius kinetic energy was first proposed by a Dutch chemist J.H. van't Hoff in 1884 and was justified by Swedish chemist Svante Arrhenius in 1889 5 years later [32]. This equation is remarkably accurate for the dependency of temperature with the reaction rate constant. It can be seen as the best empirical relationship in modeling temperature variance coefficient.

An increase of 10 degree Celsius doubles the reaction rate which is supported by Arrhenius. The higher the collision rate results higher kinetic energy and higher activation energy. The amount of energy required to ensure reaction happens is the

activation energy. Upon collision, this energy can be used to bend and break bonds leading to chemical reactions.

Activation energy can be regarded as the height of the potential barrier or energy barrier separating between the potential energy of reactants and the product of reactions. There should be a correct number of molecules with energy equal or greater than the activation energy.

In some cases, rates of reaction decreases with increasing temperature. This can be related with barrier less reactions, in which the reaction proceeding relies on the capture of molecules in a potential well. Increasing temperature leads to a reduced of collision is expressed as a reaction cross section that decreases with increasing temperature

Also, the kinetic energy can be related to chemical thermodynamics study of the interrelation of heat and with chemical reactions. The thermodynamics potential are the quantitative measures of energy stored as they evolve from an initial state to the final state. The fundamental laws of the four equations or called 'fundamental Gibbs free energy' are typically used in order to predict the energy exchanges.

Arrhenius equation demonstrated that,

$$k = Ae^{-E_a/RT}$$

where E_a is the activation energy,

$$R = 8.314 \times 10^{-3} \text{ kJ mole}^{-1} \text{ K}^{-1}$$

T = temperature in Kelvin,

A = proportionality constant

Taking the natural logarithm of Arrhenius equation gives,

$$\ln(k) = -(E_a/R)(1/T) = \ln(A)$$

$$y = mx = b$$

Plot $\ln(k)$ vs $1/T$ and the data will give a straight line and by determining the slope, the value of activation energy can be calculated

With a catalyst, the activation energy will be lowered without changing the product energy. This is shown in the figure below. With positive activation energy, the reaction is endothermic which it absorbs heat from the surroundings.

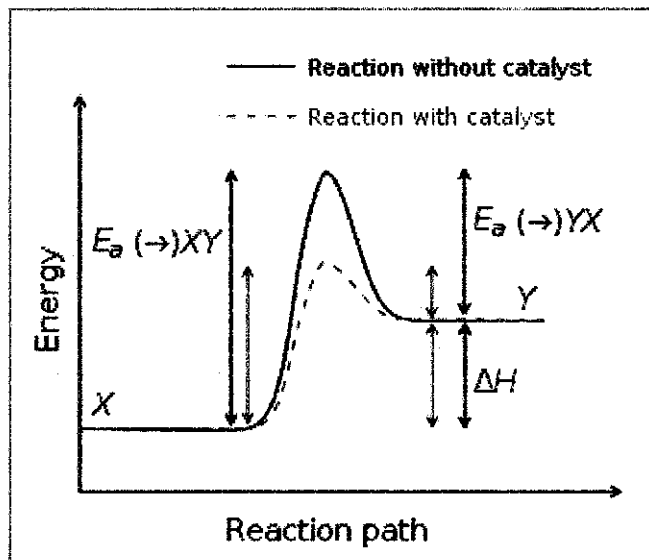


Figure 5: Activation energy

2.9 Gibbs Free Energy

Gibbs free energy is equal to the work of the system in exchanging with its surroundings after subtracting the work of forces during the transformation from initial state to final state.

It was developed by Josiah Willard Gibbs in the 1870s which he described it as the 'available energy'. The energy is described as the enthalpy of the system minus the product of the entropy times the temperature of the system,

$$G = H - TS$$

Therefore the change in the system during the reaction is equal to,

$$\Delta G = \Delta H - \Delta (TS) \text{ and,}$$

$$\Delta G = \Delta H - T \Delta S \text{ at constant temperature}$$

Under the standard-state free energy of reaction (ΔG°),

$$\Delta G^\circ = \Delta H^\circ - T \Delta S^\circ$$

To determine the reaction is spontaneous or not, the enthalpy and entropy terms have different sign conventions. It can be concluded by looking at the ΔG° *sign*.

Favorable or spontaneous reactions: $\Delta G^\circ < 0$

Unfavorable or non-spontaneous reactions: $\Delta G^\circ > 0$

Reactions can be classified as endothermic ($\Delta H > 0$) which it absorbs heat or exothermic ($\Delta H < 0$) which it releases heat. While reactions can also be described in term of their free energy as exergonic ($\Delta G < 0$) or endergonic ($\Delta G > 0$) where the free energy either increases or decreases during the reaction.

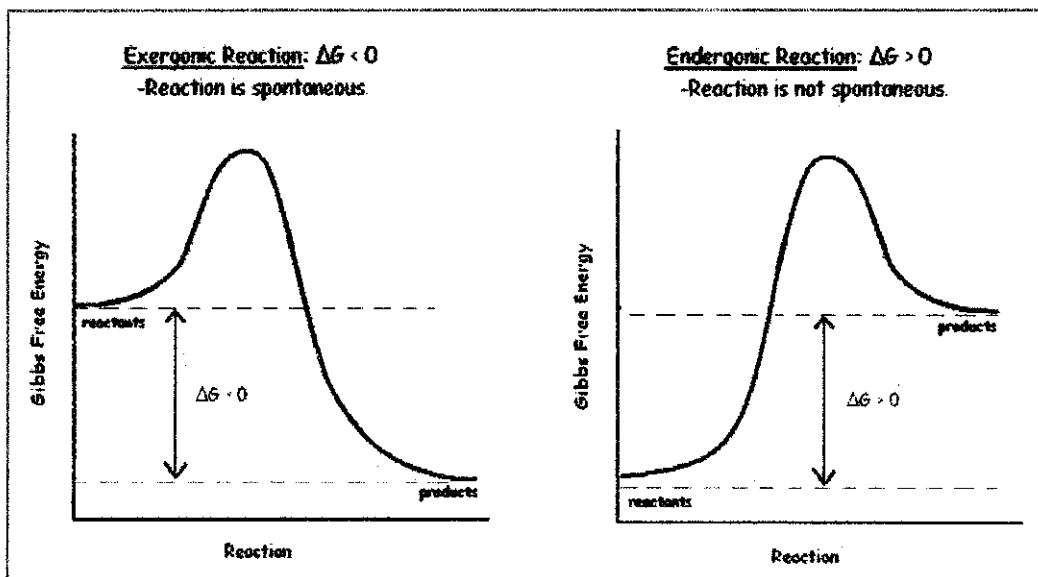


Figure 6: Gibbs free energy

CHAPTER 3

METHODOLOGY

3.1 Procedure Identification

The project execution flow is shown in Figure 7.

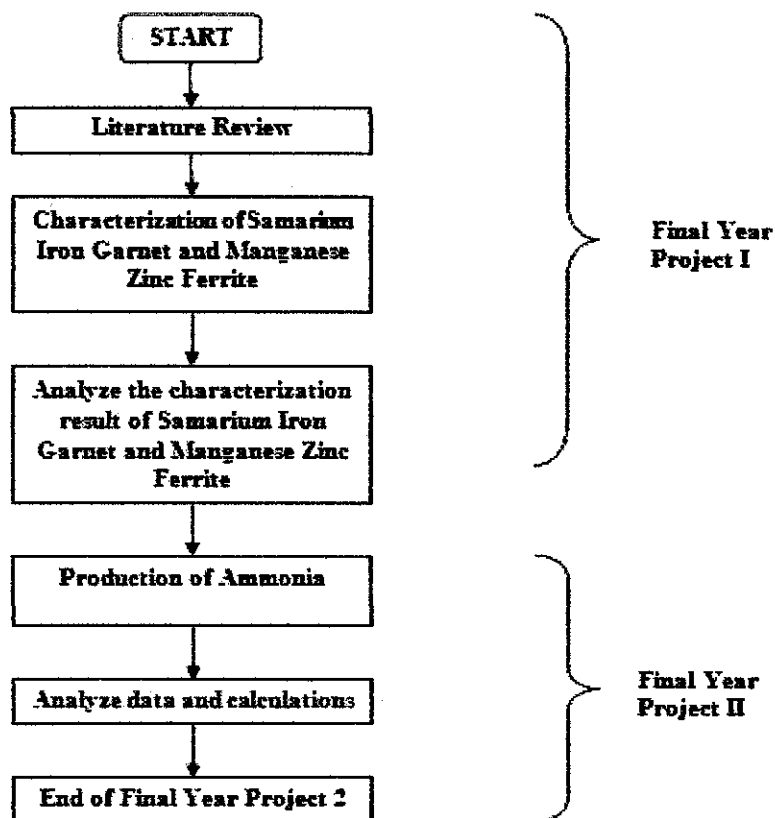


Figure 7: Flow chart of the project

There are several steps involved upon completing this project which can be divided into five main parts

- Research and literature review
- TPR for Samarium Iron Garnet, Yttrium Iron Garnet and Manganese Zinc Ferrite
- Preliminary experiments in the lab
- Collection of Ammonia

The first part of this project is devoted into studying the research paper and literature review. Topics including Manganese Zinc Ferrite and Garnet materials and other relevant theories are critically reviewed. This is essential to get an overview of the ammonia production before further determining the good catalyst in producing ammonia.

The second stage of the project will be the TPR of the catalyst of Samarium Iron Garnet, Yttrium Iron Garnet and Manganese Zinc Ferrite obtaining the 0.2 gram of the material. The TPR is done in order to reduce the oxide inside the nanocatalyst. The role of CNTs as a support will also be evaluated.

Preliminary experiments in the lab will include testing of the catalyst in the effectiveness of producing the ammonia. After testing the catalyst at different temperature from room temperature to 188°C every 30 minutes, a magnetic field should be applied to the micro reactor while producing the ammonia.

The final stage of this project is to collect the ammonia obtained after running both nitrogen and hydrogen gases through the catalyst. The data collected will then be analyzed.

3.2 Technical design

3.2.1 *Micro Reactor*

Micro reactor temperature operation ranging from 28°C to 200°C with pressure condition of 1 Bar and magnetic field of 1 Tesla is used in this experiment

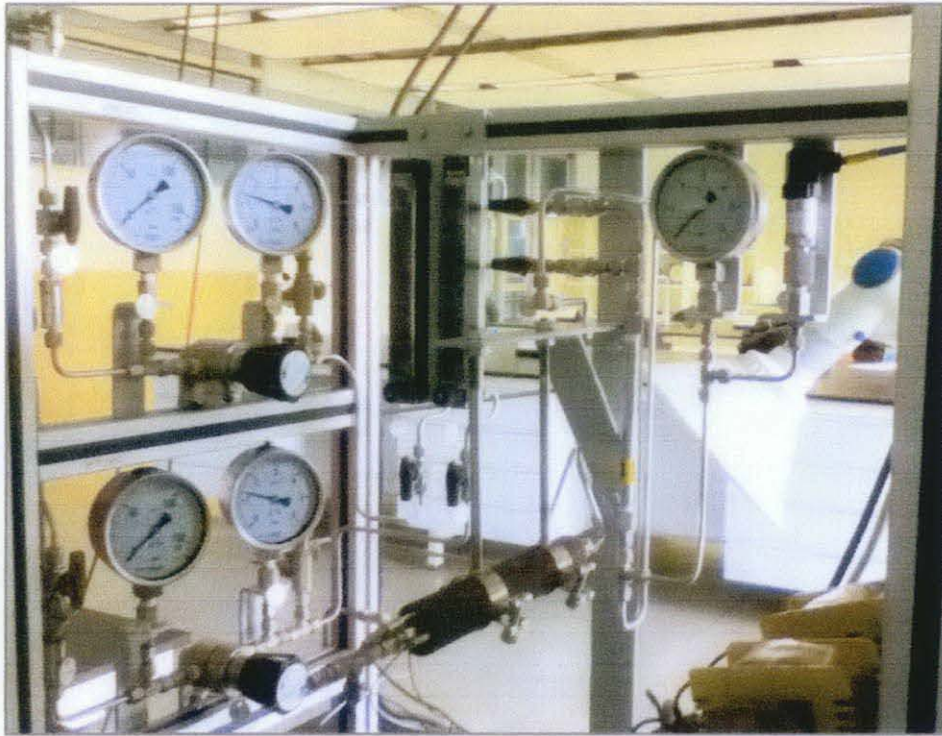


Figure 8: Micro reactor in the lab

3.2.2 *Tools and Equipments of the experiment*

3.2.2.1 *Magnetizer*

Magnetizer is used in this experiment to apply magnetic field towards the catalyst to observe the production of ammonia

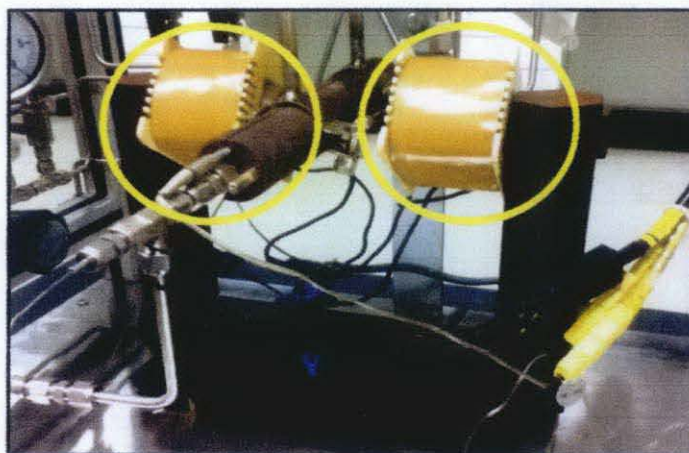


Figure 9: The magnetization coil

3.2.2.2 Kjeldahl Method

This method is applied in this experiment after varying the temperature of the microreactor from 28°C, 48°C, 68°C, 88°C, 108°C, 128°C, 148°C, 168°C, and 188°C. Then gas is flowed into 2.5mL of HCL. After 30 minutes, the gas is then collected and 5 drops of penohtalene is added and then titrate it using NaOH. The amount of NaOH used is counted to calculate the amount of ammonia produced



$$\text{HCl}_{\text{total}} = 2.5 \text{ ml}$$

$$\begin{aligned} \text{Mole HCl}_{\text{total}} &= \frac{2.5}{1000} \times 0.01M \\ &= 2.5 \times 10^{-5} \end{aligned}$$

$$\text{Amount of HCl}_{\text{reacted}} = \text{Amount of NH}_3$$

$$\text{Amount of HCl}_{\text{excess}} = \text{Amount of NaOH}$$

$$\text{Nanocatalyst} = \text{Mn}_{0.8}\text{Zn}_{0.2}\text{Fe}_2\text{O}_4 \text{ \& \ } \text{Sm}_3\text{Fe}_5\text{O}_{12} \text{ by self combustion method}$$

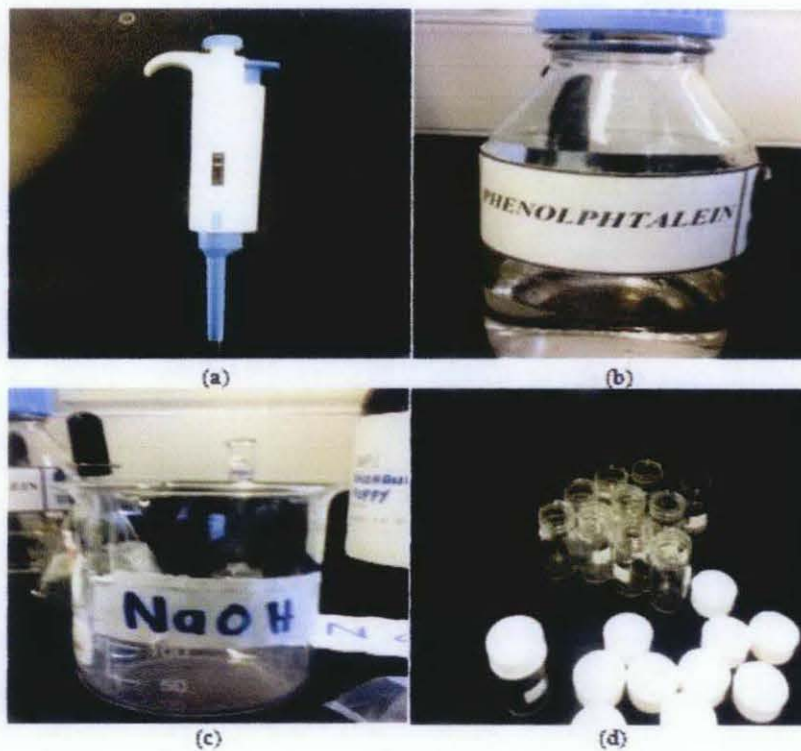


Figure 10: (a) Titration pipet; (b) Phenolphthalein; (c) NaOH; (d) Ammonia collection bottle

3.2.2.3 Tesla Coil

A total of 1 Tesla is used in this experiment.



Figure 11: Tesla Power Supply

3.2.2.4 Helmholtz

Helmholtz is set with 3.8V, 0.55A and 320 turns.



Figure 12: Helmholtz coil

CHAPTER 4

RESULTS AND DISCUSSION

4.1 SaIGs Characterization

Figure below shows the XRD spectra of the as-prepared catalyst obtained at annealing temperature of 1100°C and 1350°C

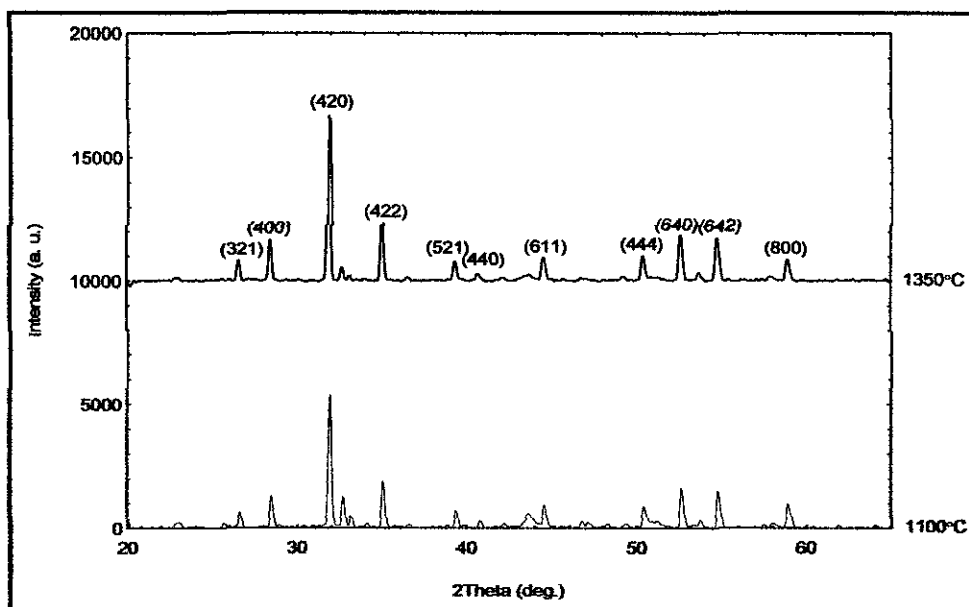


Figure 13: XRD profile calcined at different temperature

The XRD technique takes a sample of the material and places a powdered sample in a holder to determine the structure, grain size and preferred orientation. Then the sample is illuminated with x-rays of a fixed wave-length while measuring the intensity of the reflected radiation using a goniometer. This data is then analyzed and calculated using Scherrer equation which is

$$\tau = k\lambda / \beta \cos\theta$$

where,

$$k = 0.9$$

$$\lambda = 1.5406 \text{e}^{-10}$$

$$\beta = \text{FWHM} \times 2 \times \pi / 360 = 2.23 \times 10^{-3}$$

$$\theta = 32.409/2 = 16.2045$$

$$\tau = 64.76 \times 10^{-9}$$

The size of the grain is 64.76 nm. Crystallization of SaIG to form single phase occurred at temperature 1350°C.

Then SaIG was send to the lab to get the Field Emission Scanning Electron Microscopy and Energy Dispersed X-ray (FESEM). The figures show irregular shapes and agglomerated particles.

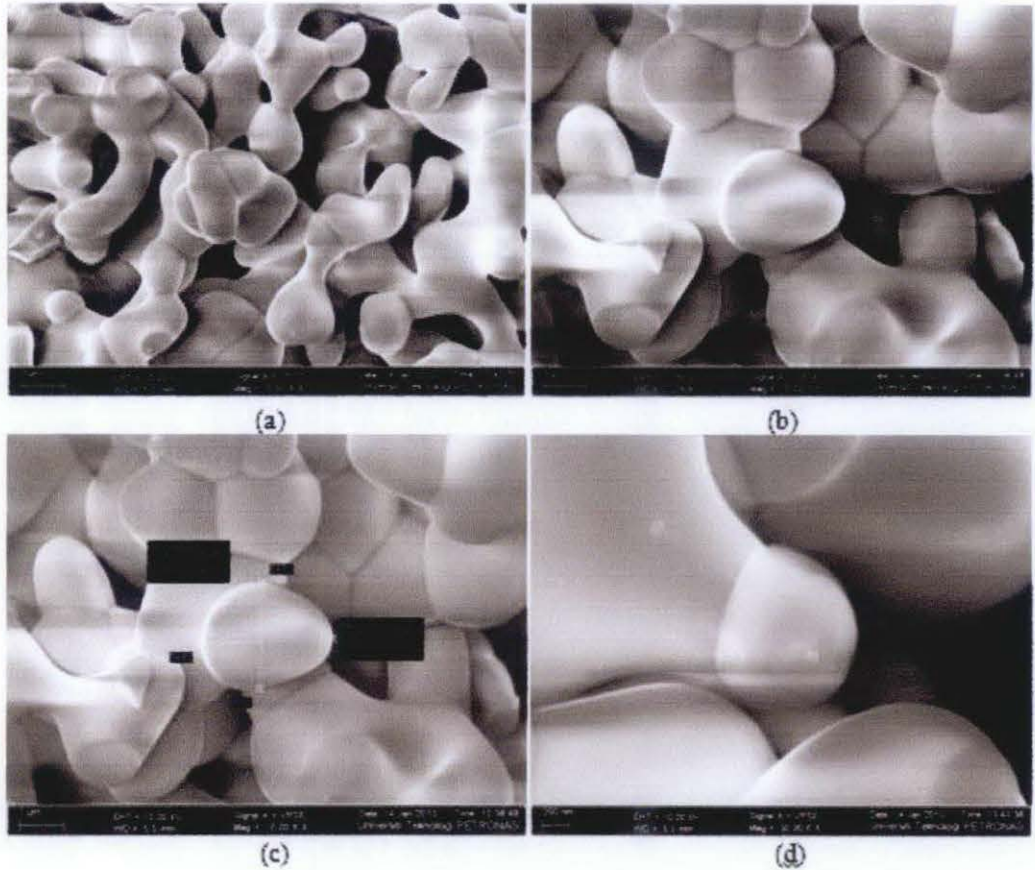


Figure 14: FESEM analysis at different resolutions

Then the sample was also taken to the lab for TPR process. The table below shows that the reduction for SaIG only occurred once at the temperature of 806°C to become metallic state. The process was run using hydrogen gas, flow 20 ccm/min, start temperature 20°C, stop temperature 800°C and hold for 15 minutes.

Table 3: TPR for SaIG

Temperature	% Hydrogen	MVs	$\mu\text{mol/g}$
806	100	284967.60	132.90691

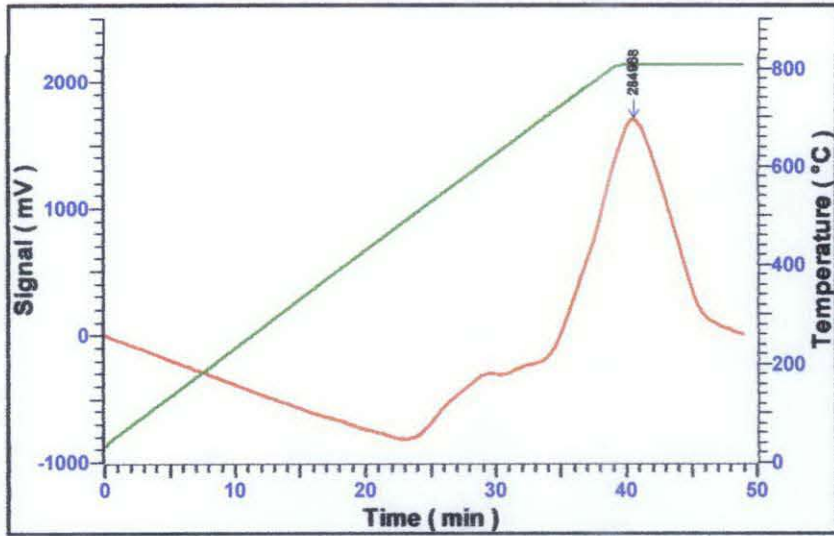


Figure 15: TPR result of SaIG (detected peak is at 284968 mVs)

Table below shows the EDX results for SaIG in term of atomic percentage, weight percentage and the standard deviation.

Table 4: EDX results of SaIG

Element	Weight%	Atomic%	Standard Deviation (%)
O K	22.53	53.84	10.26
Fe K	35.07	36.29	45.16
Sm L	42.40	9.87	34.2
Totals	100.00	100.00	

4.2 Ammonia production of SaIG, Manganese Zinc Ferrite, and YIG

When Samarium Iron Garnet is used as the catalyst, the production of ammonia can be observed by manipulating the temperature and the condition of the micro reactor which are with or without the magnetic field. The experiment is carried out using steel chamber. The results is summarized in table below

Table 5: Percentage of Ammonia yield with and without Magnetic Field using steel chamber

Temperature (°C)	Percentage yield of ammonia with Magnetic Field (%)	Percentage yield of ammonia without Magnetic field (%)
28	23.6	35.6
48	54.8	37.6
68	52	38.4
88	16.8	39.2
108	2.4	43.6
128	4	39.2
148	4	39.2
168	4	44
188	8	35.2

As the temperature increases, the amount of ammonia is lesser. The graph below shows the trend of the catalyst with and without magnetic field

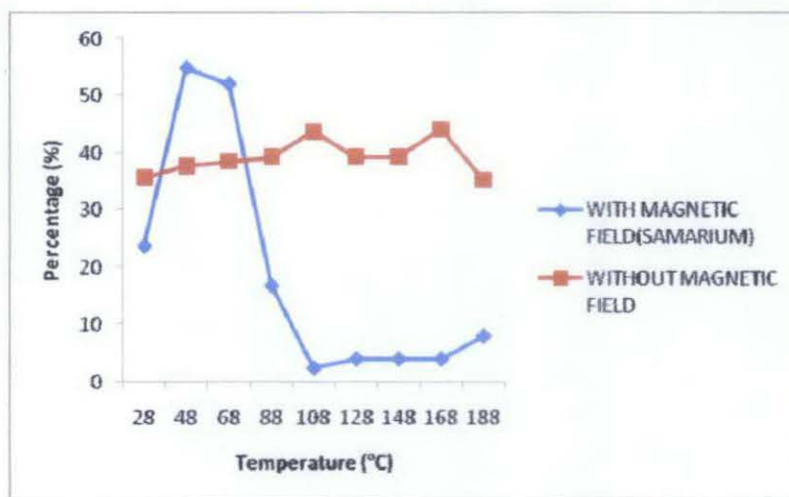


Figure 16: The graph shows that the production of ammonia decreases as the temperature increases

Based on the graph, the optimum production of ammonia is at 48°C which yielded 54.8% with the presence of magnetic field. There is an increase of yield about 45.7% in response to the magnetic field applied. In the absence of magnetic field, the yield is almost constant because there is no response of ferromagnetism towards the catalyst.

Next the catalyst is then run using glass tube at 28°C with the presence and absence of magnetic field. The results are shown in the table below

Table 6: Percentage of ammonia yield using Glass Tube at temperature of 28°C

Temperature (°C)	Percentage yield of ammonia with magnetic field	Percentage yield of ammonia without magnetic field
28	54.8%	34.8%

The trend for production of ammonia using glass tube and steel chamber is the same in room temperature, 28°C which shows the production of ammonia with magnetic field is higher. In comparison of the chamber, the glass tube produce higher amount of ammonia at room temperature. The results are summarized in the chart below

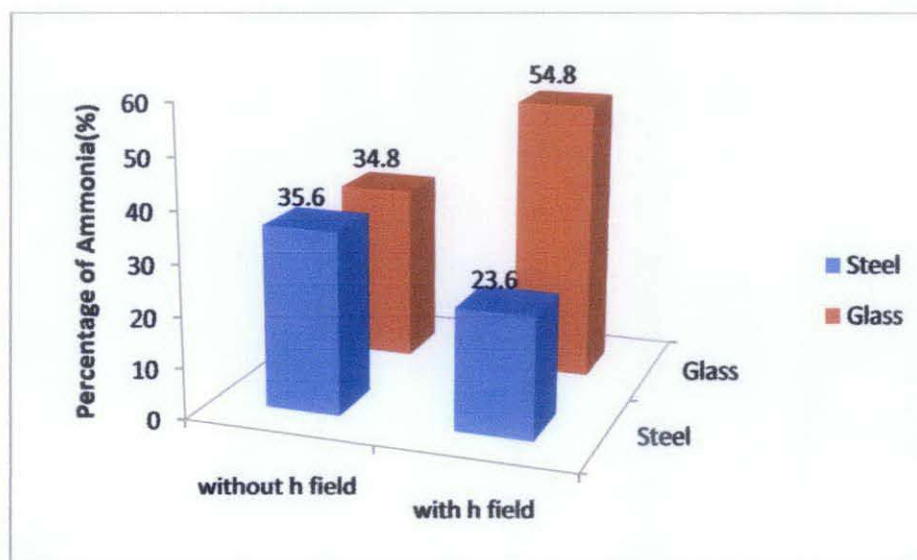


Figure 17: Comparison between steel and glass chamber

When manganese zinc ferrite were titrated the amount of ammonia obtained are listed in the table and graph below

Table 7: Percentage of Ammonia yield for Manganese Zinc Ferrite

Temperature (°C)	Percentage yield of ammonia with Magnetic Field (%)	Percentage yield of ammonia without Magnetic field (%)
28	37.6	50.8
48	33.6	51.2
68	33.6	40
88	28.4	28.4
108	44	27.2
128	35.2	26.8
148	28	26
168	43.2	25
188	47.2	25

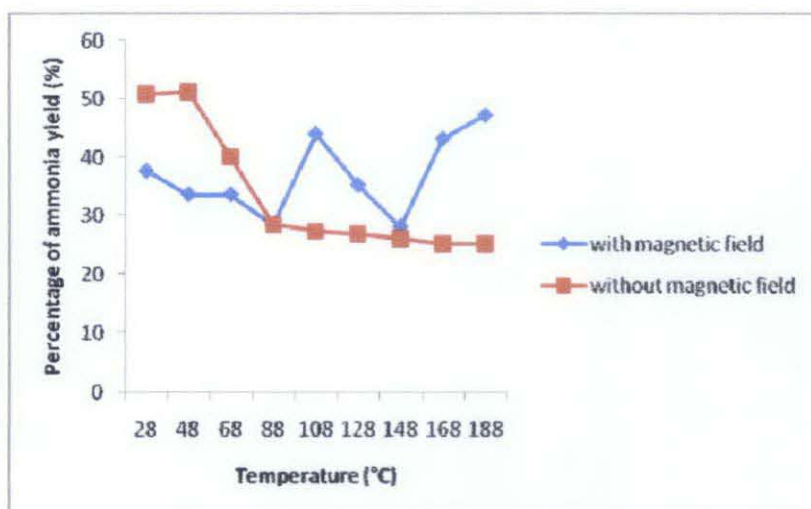


Figure 18: Production of ammonia using manganese zinc ferrite

We can observe that the production of ammonia in the absence of magnetic field is the highest at temperature of 28°C which is 50.8%. When the temperature increases, the production of ammonia is lesser. As for the amount of ammonia with the presence of magnetic field, the highest was obtained at temperature of 188°C. The trend with the presence of magnetic field is very random. We can assume that the nanocatalyst was in endothermic state from the beginning where it absorbs the energy and produce highest amount of ammonia at the temperature of 188°C.

When yttrium iron garnet was used as the nanocatalyst, the amount of ammonia obtained from the titration is listed in table and graph below

Table 8: Amount of Ammonia using YIG

Temperature (°C)	Percentage yield of ammonia with Magnetic Field (%)	Percentage yield of ammonia without Magnetic field (%)
28	62.8	51.6

48	40.8	49.2
68	38.4	44
88	20.8	44
108	17.6	31.2
128	2.4	20.8
148	4	19.6
168	1.6	23.6
188	1.2	23.7

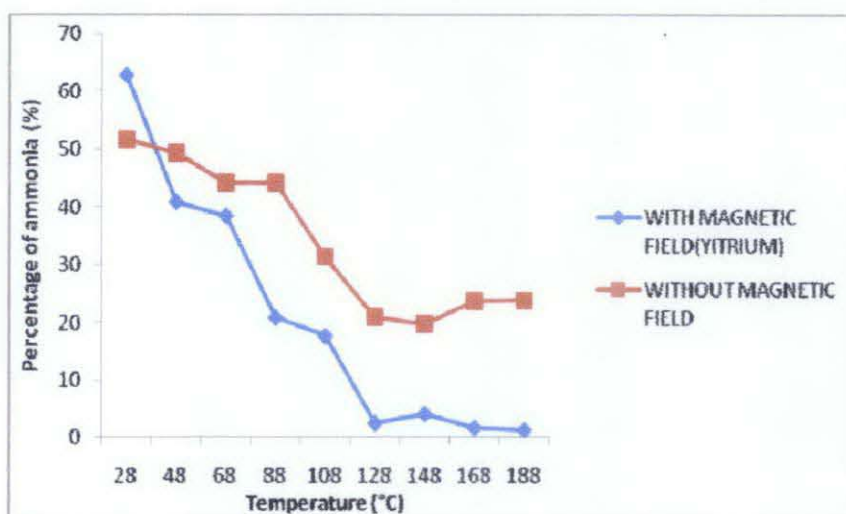


Figure 19: Production of ammonia against temperature

As the temperature increases, the amount of ammonia obtained is getting lesser. This can be explained by using the Curie temperature studies in which the

ferromagnetism of a material will decrease as the temperature increases. The optimum condition for ammonia production for YIG is at temperature 28°C with the presence of magnetic field which yielded 62.8% of ammonia production.

Out of the three nanocatalyst, the earth garnet materials gave better amount of ammonia at low temperature compared to ferrite. YIG relatively gave better amount of ammonia compared to SaIG. SaIG can serve as an alternative to YIG as nanocatalyst in producing high yield of ammonia.

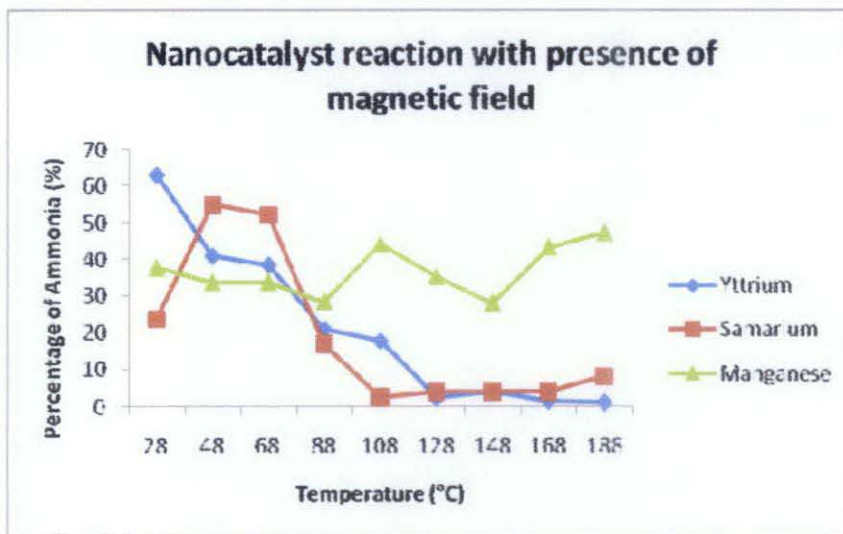


Figure 20: Three nanocatalysts in comparison (with presence of magnetic field)

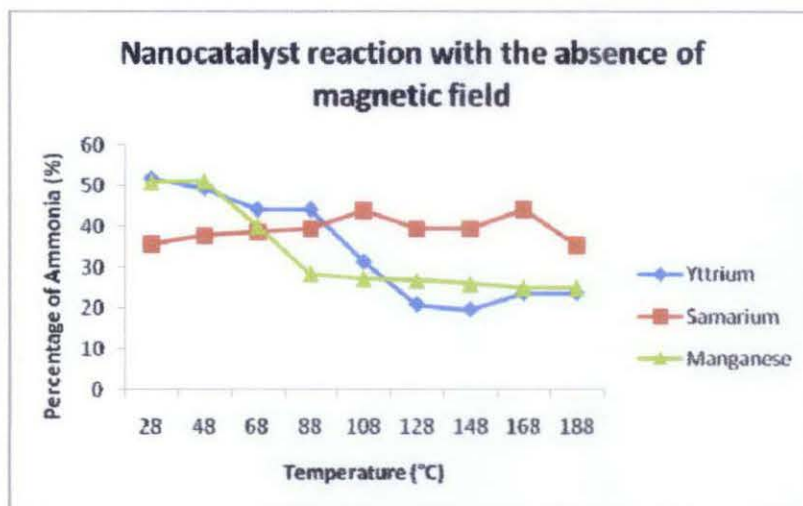


Figure 21: Three nanocatalysts in comparison (with absence of magnetic field)

The activation energy of the nanocatalyst can be determined by the Arrhenius plot. The calculation is determined based on the Temkin-Phyzev equation for ammonia synthesis. The details of the calculation are described in Appendix.

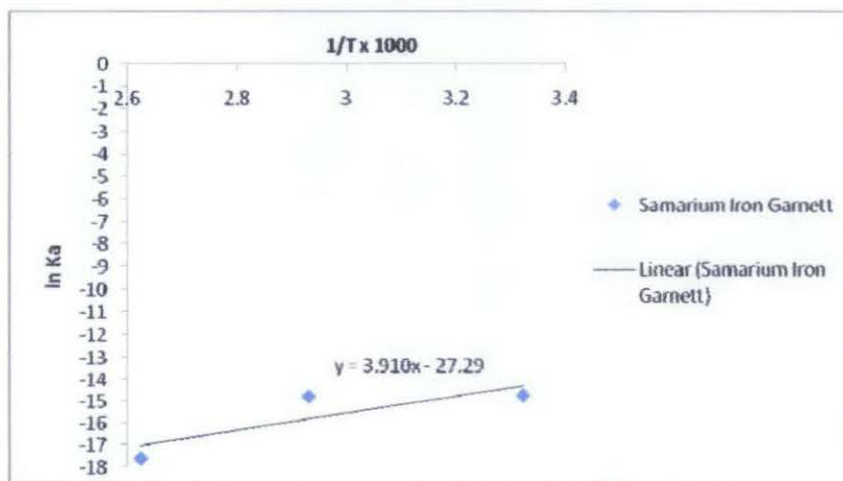


Figure 22: Arrhenius plot of ammonia production for $\text{Sm}_3\text{Fe}_5\text{O}_{12}$ nanocatalyst with magnetic field. T = 28°C - 188°C, P = 1 atm, Cat. = 0.2g, H₂:N₂ = 3:1

The activation energy, E_a was determined by calculating the gradient linear lines. In the presence of magnetic field, the calculated activation energy was 32.50 kJ/mole.

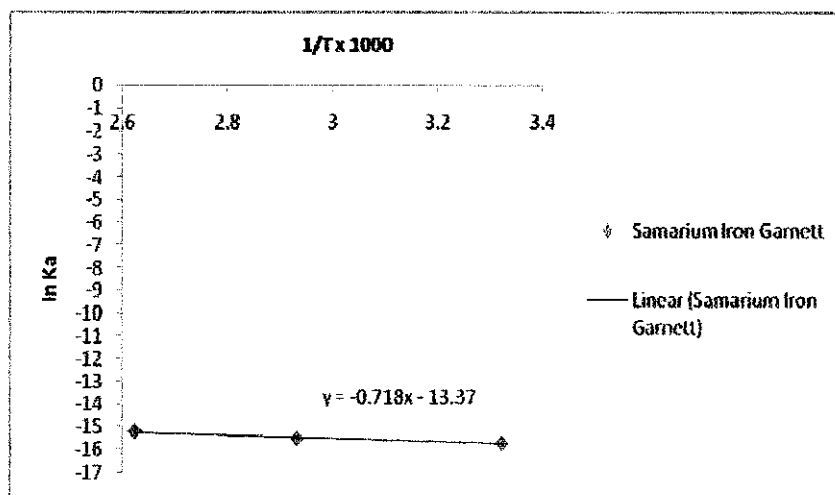


Figure 23: Arrhenius plot of ammonia production for $\text{Sm}_3\text{Fe}_5\text{O}_{12}$ nanocatalyst without magnetic field, $T = 28^\circ\text{C} - 188^\circ\text{C}$, $P = 1 \text{ atm}$, $\text{Cat.} = 0.2\text{g}$, $\text{H}_2:\text{N}_2 = 3:1$

The activation energy, E_a was determined by calculating the gradient value which is -0.718. In the absence of magnetic field, the calculated activation energy was 5.96 kJ/mole. The kinetic energy between the absence and presence of magnetic field is shown below

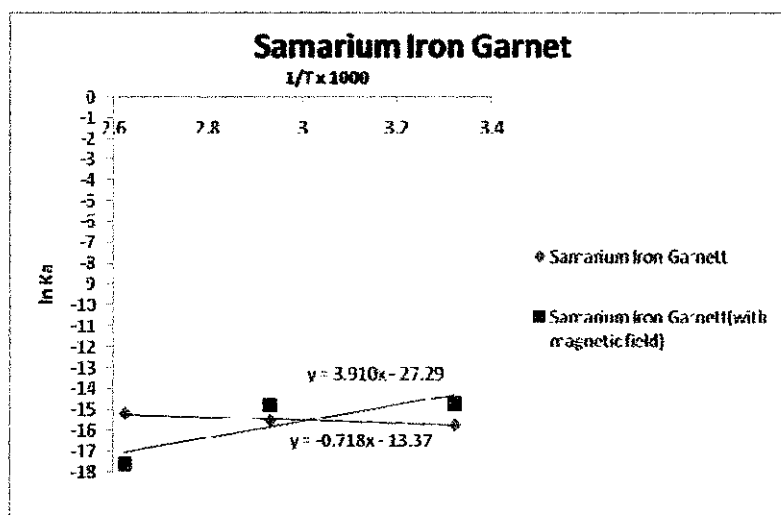


Figure 24: Production of ammonia with and without magnetic field

The activation energy for YIG can be seen through the graph below. We can observe that the activation energy for yttrium is both negative which are -8.20 kJ/mole and -43.23 kJ/mole. Both are exothermic which means it releases heat to the surrounding.

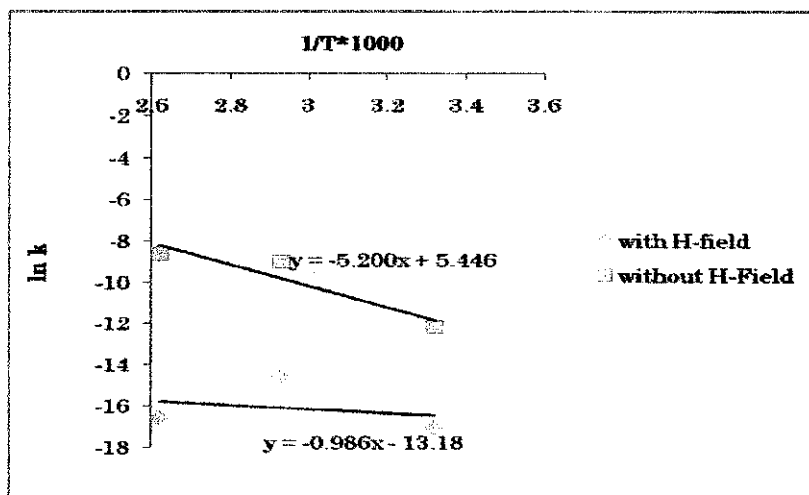


Figure 25: Activation energy for yttrium is calculated using the slope

Table below summarizes the activation for both garnet materials. YIG are exothermic in both cases while SaIG is endothermic with magnetic field and exothermic without magnetic field. With the presence of magnetic field, the amount of ammonia is higher since it is in an endothermic state which allows the transfer of electron and pairing much easier between the catalyst and reactant. An increase of 45.7% is observed when magnetic field is applied towards SaIG.

Table 9: Activation energy for both garnet materials

Material	Ea with H-Field	Ea without H-Field
Yttrium Iron Garnet	-8.20 kJ/mole	-43.23 kJ/mole
Samarium Iron Garnet	32.51 kJ/mole	-5.97 kJ/mole

Based on the results, we can see that using glass chamber gave better results compared to steel chamber. Next, we run the catalyst inside a glass chamber using both Magnetizer and Helmholtz. The result is shown in the graph. Using Magnetizer gave slightly better amount of ammonia since it gave a hard magnetic field towards the catalyst.

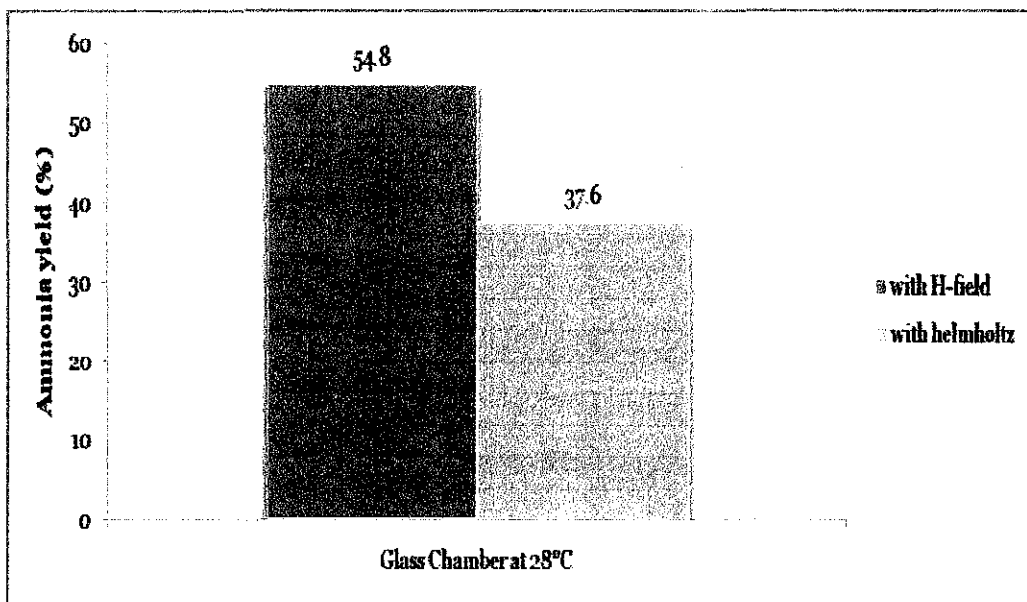


Figure 26: Comparison between Helmholtz and magnetizer as the source of magnetic field at room temperature using glass chamber

Lastly, the catalyst is then run using steel chamber with 0.1g of CNTs in the presence of magnetic field to see the effect of CNTs as a support. CNTs as a support can give the possibility to control porosity and surface chemistry of the catalyst. The results is shown in graph below

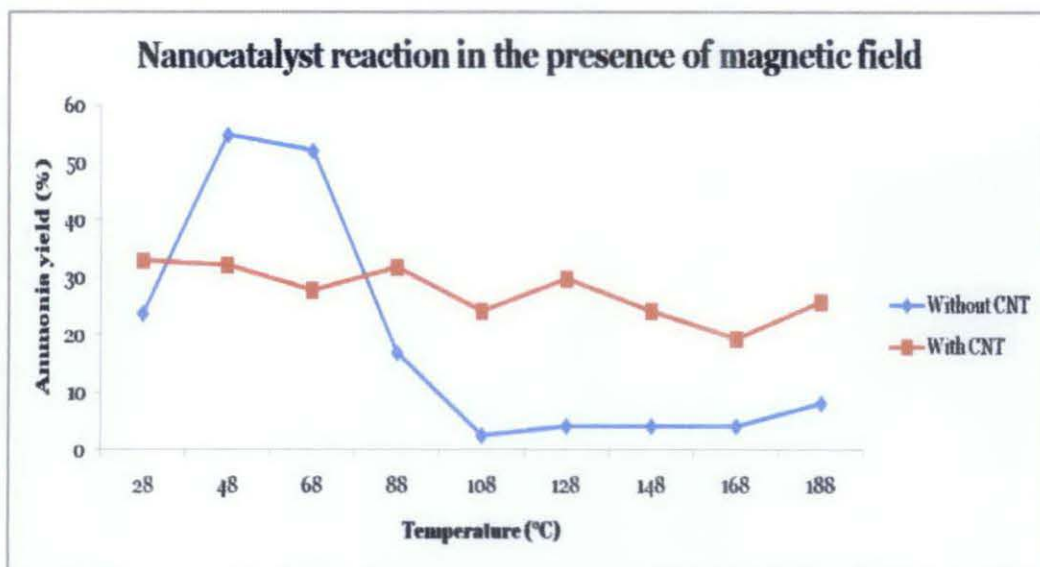


Figure 27: Ammonia yield when CNTs are mix with the catalyst

With CNTs, the highest yield is 32.8% while without CNTs is 54.8%. There is a decrease around 20% but must be noted that less catalyst is used (by 50%).

CHAPTER 5

CONCLUSION AND RECOMMENDATIONS

5.1 Conclusion

Based on the research done, the production of ammonia is done using a micro reactor system that works in low temperature (28 - 200°C), low pressure (150 – 300 atm) with higher yield of ammonia. The catalyst used in this project is Samarium Iron Garnet ($\text{Sm}_3\text{Fe}_5\text{O}_{12}$) which was reduced using TPR. This catalyst is then run by nitrogen and hydrogen gas for 30 minutes from room temperature until 188°C. The data collected from the experiment shows that with the existence of magnetic field and at temperature 48°C, the production of ammonia reaches 54.8% which is considered the optimum condition. Also, SaIG can serve as an alternative to YIG since production of ammonia is higher with garnet material compared to ferrite oxide. The amount of ammonia is higher when magnetic field is applied due to the spinning factor which allows the transfer of electron much easier [33].

5.2 Recommendations

The way forward for this project will be mixing CNTs with the catalyst to observe the effect of CNTs in ammonia production. Since with small magnetic field gave higher amount of ammonia, varying the magnetic field can give better effects of

ferromagnetism towards the catalyst hence give higher yield of ammonia. A Helmholtz can be use to replace the Magnetizer where we can manipulate the frequency since varying the current is much easier. Lastly, instead of using Kjeldahl method to obtain the amount of ammonia, a gas chromatograph can be use to check the percentage of ammonia yield.

REFERENCES

- [1] R. Schlogl, *Angew. Chem. Int. Ed.* 42 2004 (2003)
- [2] K. Tamaru, in: J. R Jennings (Ed.). *Catalytic Ammonia Synthesis*. Plenum Press, New York,(Chapter 1) (1991)
- [3] F. Garbassi, G. Fagherazzi, M. Calcaterra. *J. Catalyst Vol.* 26, pp338 (1972)
- [4] J. Pernicone, F. Ferrero, Z. Rosetti, L. Forni, P. Canton, P. Rinello, G. Fagherazzi, M. Signorot J. Pinna. *Applied Catalysis A: General Vol.* 251, pp121-129 (2003)
- [5] O. Hinrichsen. *Kinetic Simulation of Ammonia Synthesis Catalyzed by Ruthenium. Catalysis Today Vol.* 53, pp177-188 (1999)
- [6] A. Ozaki. *Acc. Chemical Resc Vol.* 14, pp16 (1981)
- [7] Pietro Moggi, Giancarlo Albanesi, Giovanni Predieri, Giuseppe Spoto. *Ruthenium Cluster-Derived Catalysts for Ammonia Synthesis. Applied Catalysis A: General Vol.* 123, pp145-159 (1995)
- [8] W.R Pilecka, E. Mi Skiewicz, D. Szmigiel, Z. Kowalezyk. *Journal of Catalysis Vol.* 231, pp11-19 (2005)
- [9] A.V. Nazarov, D. Me´nard, J.J. Green, C.E. Patton, G.M. Argentina, H.J. Van Hook, *J. Appl. Phys.* 94, 7227 (2003)
- [10] T. Aichele, A. Lorenz, R. Hergt, P. Gornet, *Cryst. Res. Technol.* 38, 575 (2003)

- [11] S. Thongmee, P. Winotai, I.M. Tang, *Solid State Commun.* 109, 471 (1999)
- [12] M.S. Lataifeh, *J. Phys. Soc. Japan* 69 (7), 2280 (2000)
- [13] M.J. Geselbrache, A.M. Cappellari, A.B. Ellis, M.A. Rzeznik, B.J. Johnson, *J. Chem. Educ.* 71 (8), 696 (1994)
- [14] M.S. Lataifeh, A. Al-Sharif, *Appl. Phys. Mater. Sci. Process A* 61, 415 (1995)
- [15] M.S. Lataifeh, A.D. Lehlooh, S. Mahmoud, *Hyperfine Interactions 3&4*, 253 (1999)
- [16] R. Nave, <http://hyperphysics.phy-astr.gsu.edu/HBASE/Solids/ferro.html>, November 10, (2009)
- [17] D.C. Tsui, H.L. Stormer, A.C. Gossard, *Phys. Rev. Lett.* 48, 1559 (1982)
- [18] R.B. Laughlin, *Phys. Rev. Lett.* 50, 1395 (1983)
- [19] T. Chakraborty, P. Pietilainen, *The Quantum Hall Effects*, Springer, Berlin, 1995; T. Chakraborty, P. Pietilainen, in: S. Das Sarma, A. Pinczuk (Eds.), *Perspectives in Quantum Hall Effects*, Wiley, New York, (1997)
- [20] B.I. Halperin, *Helv. Phys. Acta* 56, 75 (1983)
- [21] T. Chakraborty, F.C. Zhang, *Phys. Rev. B* 29, 7032 (1984)
- [22] T. Chakraborty, P. Pietilainen, F.C. Zhang, *Phys. Rev. Lett.* 57, 130 (1986)
- [23] R.J. Haug, K.v. Klitzing, R.J. Nicholas, J.C. Maan, G. Weimann, *Phys. Rev. B* 36, 4528 (1987)
- [24] K. Park, J.K. Jain, *Phys. Rev. Lett.* 80, 4237 (1998)

- [25] J.P. Eisenstein, H.L. Stormer, L. Pfeiffer, K.W. West, Phys. Rev. Lett. 62 (1989) 1540; J.P. Eisenstein, H.L. Stormer, L.N. Pfeiffer, K.W. West, Phys. Rev. B 41, 7910 (1990)
- [26] L.W. Engel, S.W. Hwang, T. Sajoto, D.C. Tsui, M. Shayegan, Phys. Rev. B 45, 3418 (1992)
- [27] R.R. Du, A.S. Yeh, H.L. Stormer, D.C. Tsui, L.N. Pfeiffer, K.W. West, Phys. Rev. Lett. 75, 3926 (1995)
- [28] I.V. Kukushkin, K.v. Klitzing, K. Eberl, Phys. Rev. Lett. 82, 3665 (1999)
- [29] I.V. Kukushkin, J.H. Smet, K.v. Klitzing, K. Eberl, Phys. Rev. Lett. 85, 3688 (2000)
- [30] G.S. Boebinger, A.M. Chang, H.L. Stormer, D.C. Tsui, Phys. Rev. Lett. 55, 1606 (1985)
- [31] R.L. Willett, H.L. Stormer, D.C. Tsui, A.C. Gossard, J.H. English, Phys. Rev. B 37, 8476 (1988)
- [32] S. Arrhenius, Z. Phys. Chem. 4, 226 (1889)
- [33] A.F. Dethlefsen et. al., Physica E., August 10, (2006)

APPENDICES

APPENDIX A

CALCULATION OF ACTIVATION ENERGY

Formula

B.1. Rate of Ammonia Production

$$\begin{aligned}\text{Rate} &= \text{mole of ammonia produced} / (\text{mass of catalyst (g)} \times \text{duration of reaction (t)}) \\ &= \text{mole}_{\text{NH}_3} / \text{g}_{\text{cat}} \cdot \text{h}\end{aligned}$$

B.2. K_A and K_B [89]

Based on equations proposed by Aparicio et al. [89] at $T = 251^\circ\text{C}$ and $P = 1 \text{ atm}$

$$K_A = 3.289 \exp [(50690 \text{ J/mol})/RT]$$

$$K_B = 7.35 \times 10^{12} \exp [(-59040 \text{ J/mol})/RT]$$

Where,

K_A = Rate constant for the formation of ammonia

K_B = Rate constant for the decomposition of ammonia

B.3. Vant Hoff's Equation [9]

$$\ln (K_{T_2}/K_{T_1}) = \Delta H/R (1/T_1 - 1/T_2)$$

Where,

T = Temperature (K)

ΔH = Heat of ammonia production = -92 kJ/mole

R = Gas constant (J/mol.K) = 8.314 J/mole.K

B.4. Ideal Gas Law [9]

$$PV = nRT$$

Where,

P = Pressure (atm)

V = Volume (L)

R = Gas constant = 0.0821 L.atm/mol. K

n = Number of mole

T = Temperature (K)

B.5. Mole fraction of component [9]

X_A = no. mol A / (Σ mol of all components)

B.6. Partial pressure of reactant/product [9]

P_A = $X_A \times P_{\text{Total}}$

Where,

P_A = Partial pressure of component A

X_A = Mole fraction of A

P_T = Total pressure

B.7. Temkin-Phyzev Equation [89], [100]

Rate (mole_{NH₃}/g_{cat}.h) = $k_A P_{N_2} [(P^3_{H_2}) / (P^2_{NH_3})]^\alpha - k_B [(P^2_{NH_3}) / (P^3_{H_2})]^{1-\alpha}$

B.8. Arrhenius equation

k = $Ae^{-E_a/RT}$

$\ln k$ = $\ln A - E_a/RT$

Where,

k = Rate constant

A = Exponential factor

E_a = Activation energy

T = Temperature (K)

Calculation

Determination of reference k_A , k_B and K_{eq} .

Based on work done by Aparicio et al. [89] at $T = 251$ °C and $P = 1$ atm, using Equation

B.2:

$k_A = 3.289 \exp [(50690 \text{ J/mol}) / 8.314 \times (251+273)]$

$= 3.717 \times 10^5$

$k_B = 7.35 \times 10^{12} \exp [(-59.04 \text{ kJ/mol}) / 8.314 \times (251+273)]$

$= 9.568 \times 10^6$

$K_{eq} = K_R = k_A/k_B = 0.038$

Hematite, $\alpha\text{-Fe}_2\text{O}_3$ nanocatalyst in the presence of magnetic field.

$$T = 30^\circ\text{C} [T_1 = 30 \quad T_2 = 251 \text{ (R)}]$$

A. Rate of Ammonia Production

Using Equation B.1:

$$\begin{aligned}\text{Rate} &= (300 \mu\text{mole} \times 1 \times 10^{-6}) / (0.2 \text{ g} \times 0.5 \text{ h}) \\ &= 3.0 \times 10^{-3} \text{ mole}_{\text{NH}_3} / \text{g}_{\text{cat}} \cdot \text{h}\end{aligned}$$

B. Determination of K_{30}

Using Equation B.3:

$$\ln (K_{30}/0.038) = (92000 / 8.314) \times (1.391 \times 10^{-3})$$

$$\ln K_{30}/0.038 = 15.40$$

$$e^{\ln K_{30}/0.038} = e^{15.40}$$

$$K_{30}/0.038 = 4.876 \times 10^6$$

$$K_{30} = 1.853 \times 10^5$$

C. Determination of P_A

Mole of fed N_2 and H_2

Using Equation B.4:

$$\begin{aligned}n_{\text{N}_2} &= PV/RT \\ &= (1.2 \text{ atm} \times 0.01 \text{ L}) / (0.0821 \text{ L}\cdot\text{atm}/\text{mol}\cdot\text{K} \times 301 \text{ K}) \\ &= 4.920 \times 10^{-4} \text{ mole}\end{aligned}$$

$$\begin{aligned}n_{\text{H}_2} &= (1.2 \text{ atm} \times 0.03 \text{ L}) / (0.0821 \text{ L}\cdot\text{atm}/\text{mol}\cdot\text{K} \times 301 \text{ K}) \\ &= 1.476 \times 10^{-3} \text{ mole}\end{aligned}$$

$$n_{\text{NH}_3} \text{ obtained} = 300 \mu\text{mole} = 3 \times 10^{-4} \text{ mole}$$

Using equation B.5:

$$\begin{aligned}X_{\text{N}_2} &= (4.920 \times 10^{-4} \text{ mole}) / [(4.920 \times 10^{-4} + 1.476 \times 10^{-3} + 3 \times 10^{-4}) \text{ mole}] \\ &= 0.216\end{aligned}$$

$$\begin{aligned}X_{\text{H}_2} &= (1.476 \times 10^{-3} \text{ mole}) / [(4.920 \times 10^{-4} + 1.476 \times 10^{-3} + 3 \times 10^{-4}) \text{ mole}] \\ &= 0.650\end{aligned}$$

$$\begin{aligned}X_{\text{NH}_3} &= (3 \times 10^{-4} \text{ mole}) / [(4.920 \times 10^{-4} + 1.476 \times 10^{-3} + 3 \times 10^{-4}) \text{ mole}] \\ &= 0.130\end{aligned}$$

Using equation B.6:

$$P_{N_2} = 0.216 \times 1 \text{ atm} = 0.216 \text{ atm}$$

$$P_{H_2} = 0.650 \times 1 \text{ atm} = 0.650 \text{ atm}$$

$$P_{NH_3} = 0.130 \times 1 \text{ atm} = 0.130 \text{ atm}$$

D. Determination of k_A

$$\text{Rate (mole}_{NH_3}/g_{cat}\cdot h) = k_A P_{N_2} [(P_{H_2}^3)/(P_{NH_3}^2)]^{\alpha} - k_B [(P_{NH_3}^2)/(P_{H_2}^3)]^{1-\alpha}$$

Using Equation B.7:

$$3 \times 10^{-3} = k_A(0.216)[(0.65)^3/(0.13)^2]^{0.75} - k_B[(0.13)^2/(0.65)^3]^{1-0.75}$$

$$3 \times 10^{-3} = 1.74 k_A - 0.49 k_B$$

$$= 1.74 k_A - 0.49 (k_A/K_{30})$$

$$k_A = 1.724 \times 10^{-3}$$

APPENDIX B

TABLE FOR ACTIVATION ENERGY CALCULATIONS

SAMARIUM IRON GARNET WITH THE PRESENCE OF MAGNETIC FIELD

TEM P	MOLE(μ)	RATE	nN2	nH2	nNH3	XN2	XH2	XNH3	pN2	pH2	pNH3	Keq	Ka	In Ka
28	13.1	0.0001 31	0.0004 92	0.0014 76	0.00001 31	0.2483 47	0.7450 41	0.0066 12	0.2483 47	0.7450 41	0.0066 12	2370 00	3.88257 E-07	- 14.76 16
68	13	0.0001 3	0.00049 2	0.0014 76	0.00001 3	0.2483 59	0.7450 78	0.0065 62	0.2483 59	0.7450 78	0.0065 62	3174	3.80861 E-07	- 14.78 08
108	4.2	0.0000 42	0.00049 2	0.0014 76	0.00000 42	0.2494 68	0.7484 03	0.0021 3	0.2494 68	0.7484 03	0.0021 3	105.2	2.24456 E-08	- 17.61 22

SAMARIUM IRON GARNET WITH THE ABSENCE OF MAGNETIC FIELD

TEM P	MOLE(μ)	RATE	nN2	nH2	nNH3	XN2	XH2	XNH3	pN2	pH2	pNH3	Keq	Ka	In Ka
28	8.9	0.0000 89	0.0004 92	0.0014 76	0.00000 89	0.2488 75	0.7466 24	0.0045 02	0.2488 75	0.7466 24	0.0045 02	2370 00	1.47243 E-07	- 15.73 12
68	9.6	0.0000 96	0.0004 92	0.0014 76	0.00000 96	0.2487 86	0.7463 59	0.0048 54	0.2487 86	0.7463 59	0.0048 54	3174	1.7802E -07	- 15.54 14
108	10.9	0.0001 09	0.0004 92	0.0014 76	0.00001 09	0.2486 23	0.7458 69	0.0055 08	0.2486 23	0.7458 69	0.0055 08	105.2	2.44784 E-07	- 15.22 29

YTTRIUM IRON GARNET WITH THE PRESENCE OF MAGNETIC FIELD

TEM P	MOLE(μ)	RATE	nN2	nH2	nNH3	XN2	XH2	XNH3	pN2	pH2	pNH3	Keq	Ka	In Ka
28	19.1	0.0001 91	0.0004 85	0.0014 5	1.91E- 05	0.2481 96	0.7420 3	0.0097 74	0.2481 96	0.7420 3	0.0097 74	2370 00	1.02712 E-06	- 13.78 88
68	12	0.0001 2	0.0004 28	0.0012 85	0.0000 12	0.2481 16	0.7449 28	0.0069 57	0.2481 16	0.7449 28	0.0069 57	6500 0	3.84169 E-07	- 14.77 22
108	24.4	0.0002 44	0.0003 83	0.0011 5	2.44E- 05	0.2459 23	0.7384 1	0.0156 67	0.2459 23	0.7384 1	0.0156 67	729	2.71085 E-06	- 12.81 82

YTTRIUM IRON GARNET WITH THE ABSENCE OF MAGNETIC FIELD

TEM P	MOLE(μ)	RATE	nN2	nH2	nNH3	XN2	XH2	XNH3	pN2	pH2	pNH3	Keq	Ka	In Ka
28	12.9	0.0001 29	0.0004 85	0.0014 5	1.29E- 05	0.2489 86	0.7443 91	0.0066 23	0.2489 86	0.7443 91	0.0066 23	2370 00	3.83213 E-07	- 14.77 47
68	11	0.0001 1	0.0004 28	0.0012 85	0.0000 11	0.2482 6	0.7453 6	0.0063 81	0.2482 6	0.7453 6	0.0063 81	6500 0	3.08797 E-07	- 14.99 06
108	7.8	0.0000 78	0.0003 83	0.0011 5	7.8E-06	0.2485 72	0.7463 66	0.0050 62	0.2485 72	0.7463 66	0.0050 62	729	1.5413E -07	- 15.68 55